Effect of α-Fe impurities on the field dependence of magnetocaloric response in LaFe$_{11.5}$Si$_{1.5}$

CrossMark

J.S. Blázquez [a, *], L.M. Moreno-Ramírez [a], J.J. Ipus [a], L.F. Kiss [b], D. Kaptás [b], T. Kemény [b], V. Franco [a], A. Conde [a]

[a] Dpto. Física de la Materia Condensada, Universidad de Sevilla, ICMSE-CSIC. P.O. Box 1065, 41080 Sevilla, Spain
[b] Wigner Research Centre for Physics, Hungarian Academy of Sciences, P.O.Box 49, 1525 Budapest, Hungary

A R T I C L E   I N F O

A B S T R A C T

In this work, the theoretical field dependence of the magnetic entropy change far away from the transition is used to analyze the field dependence of composite materials formed by fcc La(Fe,Si)$_{13}$ and bcc α-Fe(Si) phases. A non-interacting phases approximation is followed in the analysis and results are in good agreement with microstructural data obtained from X-ray diffraction and Mössbauer spectroscopy. The range of validity of the approximation is estimated. It is concluded that the quadratic field dependence of magnetic entropy change is reached a few tens of kelvin above the transition temperature at 1.5 T. However, the linear dependence (characteristic of ferromagnets well below its Curie temperature) is only reached a few hundred kelvin below the transition. The results presented here can be used in the deconvolution of the contribution of impurities to the MCE signal in composites.

© 2015 Elsevier B.V. All rights reserved.

1. Introduction

Magnetocaloric effect (MCE) is a hot topic due to the perspective of its application in room temperature magnetic refrigeration technology. This scientific interest rose up especially after the works of Gschneidner Jr. and Pecharsky, who found giant MCE in Gd$_5$Si$_2$Ge$_2$ compound at 292 K [1]. Since then other systems, such as Heusler alloys [2], La(FeSi)$_{13}$H$_δ$ [3] or MnAs [4] compounds and previously FeRh [5], were found to exhibit a giant MCE too [6,7]. In general, giant MCE is associated to a first order phase transition implying structural or itinerant electron metamagnetic transitions.

In the particular case of La(Fe,Si)$_{13}$ family, Si stabilizes the NaZn$_{13}$-type phase (space group Fm3c) but the production of pure single phase samples is tricky and requires long high temperature annealing that can be reduced if the precursor alloy is well homogenized by rapid quenching [8] or milling [9]. The typical residual impurity phases are ferromagnetic bcc Fe and tetragonal weak Pauli paramagnetic LaFeSi intermetallic [10]. The presence of impurities generally leads to a decrease of the MCE response (except for cases were the minority phase has a Curie temperature below but close to that of the main phase [11–13]).

In general, the mathematical function describing the shape of the magnetic entropy change, $\Delta S_M(T,H)$, is not known but only achievable experimentally. However, some works have been devoted to the field dependence of ΔS_M proposing a power law [14,15]: $\Delta S_M = aH^n$, where the value of a is only dependent on temperature and n is field independent well below the Curie temperature, T_C, (where $n = 1$) and well above T_C (where $n = 2$). At T_C, for a second order phase transition (SOPT), n is also field independent and related to the critical exponents [15]. In this line of study, the aim of this work is to use this information about the field dependence of MCE to further analyze composite materials in order to extract the contribution of some of the phases (when they are strongly ferromagnetic or weakly paramagnetic ones). In particular, the proposed ideas will be applied to LaFe$_{11.5}$Si$_{1.5}$ alloy with α-Fe impurities, where the Curie temperatures of both phases (~250 K and ~1000 K, respectively) are well apart.

As a first approximation, the magnetic entropy change of a multiphase system can be estimated as the sum of the contributions of the independent phases, e.g. for a two phase system.

$$\Delta S_M = X\Delta S_M^{(1)} + (1 - X)\Delta S_M^{(2)} \tag{1}$$

where the superindexes correspond to the individual phases. X is the fraction of phase 1, which in the following will be considered the impurity phase.

* Corresponding author.
E-mail address: jsebas@us.es (J.S. Blázquez).

2. Experimental

Alloy of nominal composition of LaFe$_{11.5}$Si$_{1.5}$ was prepared in the form of ingots and ribbons. The ingots were fabricated via induction melting under Ar atmosphere in a cold crucible. The melting was carried out four times to ensure the homogeneity of the alloy. The weight loss during melting was less than 0.1%. The ribbons with a cross section of 0.5 mm × 15 μm were prepared by melt spinning (with a circumferential wheel speed of 40 m/s) in vacuum. The samples were annealed at 1323 K for 2 h (ribbons), 3 days and 1 week (ingots) in sealed quartz tubes under He atmosphere. During annealing, the ingots were wrapped in a Ta foil and after annealing, the quartz tubes were water quenched.

X-ray diffraction (XRD) and Mössbauer measurements were performed on pieces of ribbons and on powder samples obtained by crushing the ingots in a ceramic mortar. XRD experiments were performed using Cu-Kα radiation in a Bruker diffractometer (D8 Advance A25) and Rietveld refinement of the diffraction patterns were done using TOPAS program. The ^{57}Fe Mössbauer measurements were carried out by a conventional constant acceleration-type spectrometer at room temperature. The magnetic properties were measured on small pieces of ingots and ribbons, oriented to minimize the effect of the demagnetizing field, in a Lakeshore 7407 vibrating sample magnetometer (VSM) from 77 to 663 K, using a maximum magnetic field of 1.5 T. MCE was studied by measuring isothermal magnetization curves and applying Maxwell relation to these data. The analysis of isothermal magnetization curves was performed using the Magnetocaloric Effect Analysis Program [16,17]. Although the application of Maxwell relation can yield artifacts due to non equivalent starting points for each isothermal curve [18], these artifacts are restricted to the temperature range in which the magnetocaloric effect is hysteretic. In this study our interest is far apart from the transition and thus the possible artifacts are not affecting the analysis derived in this work.

3. Results and discussion

Fig. 1 shows the XRD patterns of the different studied samples along with the fitting curves generated from Rietveld refinement. Phase fractions in weight % are shown in Table 1. Along with the fcc La(FeSi)$_{13}$ phase, bcc Fe-type phase appears with (200) texture in the melt-spun sample. Small traces of LaFeSi cannot be discarded. The lattice parameter of the La(Fe,Si)$_{13}$ phase is slightly higher than that reported by other authors for LaFe$_{11.5}$Si$_{1.5}$ [19,20] but decreases as the amount of α-Fe phase decreases. In the case of the α-Fe phase, no significant changes are observed among the different studied samples (see Table 1). The crystal size of the fcc phase remains above 100 nm for the three studied samples as well as that of the α-Fe for the melt-spun sample. For the bulk sample annealed for 3 days at 1323 K, the α-Fe phase shows a size of 40 nm. The small amount of this phase in the sample annealed for 1 week prevents a good estimation of its crystal size in that case.

Fig. 2 shows the experimental room temperature Mössbauer spectra along with the contributions used to fit the data. A maximum of three ferromagnetic sites were used to fit the bcc α-Fe(Si) phase and a paramagnetic doublet was used to fit the contribution from the fcc La(Fe,Si)$_{13}$ phase. The fraction of Fe atoms in the bcc phase was estimated from the corresponding area ratio. The trends of the fraction of α-Fe phase obtained from XRD and Mössbauer are in good agreement (see Table 1). However, it is worth noting that Mössbauer data refer to the fraction of the total number of Fe atoms in the different phases, whereas XRD data correspond to weight % of the phase. Moreover, whereas our Mössbauer experiments study the whole sample, as it operates in

transmission mode, XRD experiments are limited to the penetration depth of the radiation in the ribbon (~9 μm, calculated from the mass absorption coefficient at the Cu Kα wavelength for this composition).

Magnetic entropy change curves are shown in Fig. 3. The trend of the magnitude of the peak is in agreement with the fraction of La(Fe,Si)$_{13}$ phase detected by XRD and Mössbauer, evidencing the deleterious effect of α-Fe impurities on the MCE of this family of alloys [8]. In fact, the presence of impurities may seriously affect the field dependence of the MCE [21]. Starting from Eq. (1), which assumes non-interacting phases, the total magnetic entropy change in a biphasic system can be written as:

$$\Delta S_M = a_1 X H^{n_1} + a_2 (1 - X) H^{n_2} \qquad (2)$$

where the entropy change of each individual phase is expressed as a power law of the field [14], prefactors a_i correspond to the magnetic entropy change of the i phase at 1 T and the exponents n_i should be field independent in the temperature regions previously described [15].

In any case, an experimental local n exponent of the biphasic system can be obtained assuming $\Delta S_M = aH^n$. This exponent n is related to the corresponding parameters a_i and n_i.

$$n = \frac{d\ln(\Delta S_M)}{d\ln(H)} = \frac{a_1 n_1 X H^{n_1} + a_2 n_2 (1 - X) H^{n_2}}{\Delta S_M} \qquad (3)$$

Two different cases can be distinguished as a function of the magnetic character of the phases.

a) In the case of paramagnetic impurities, $n_1 = 2$. Therefore, Eq. (3) can be written as:

$$n = \frac{2a_1 X H^2 + a_2 n_2 (1 - X) H^{n_2}}{\Delta S_M} = \frac{a_1 H^2}{\Delta S_M} X(2 - n_2) + n_2 \qquad (4)$$

Assuming a Curie law for the paramagnetic phase, a_1 should be proportional to T^{-2} and negligible except for very low temperatures, thus $n \sim n_2$ (in any case, as $n_2 \leq 2$, $n \geq n_2$).

b) For ferromagnetic impurities with a higher Curie temperature than that of the phase of interest (phase 2), if $T \ll T_C^{(1)}$ and $T \ll T_C^{(2)}$ both exponents n_1 and n_2 should be equal to 1 and Eq. (3) can be written as:

$$n = \frac{X a_1 H + (1 - X) a_2 H}{\Delta S_M} = 1 \qquad (5)$$

Therefore, ferromagnetic impurities would not affect the field dependence of MCE at this temperature range. However, as the temperature becomes closer to the transition of phase 2, n_2 is no longer 1 but lower and assuming that $T_C^{(1)} \gg T_C^{(2)}$ (e.g. as it occurs for α-Fe impurities in LaFe$_{13-x}$Si$_x$) $n_1 = 1$ and:

$$n = \frac{a_1 H}{\Delta S_M} X(1 - n_2) + n_2 \geq n_2 \qquad (6)$$

A particular case occurs when $T \ll T_C^{(1)}$ and $T = T_C^{(2)}$. If the phase 2 experiences a SOPT, n_2 should be field independent while $n_1 = 1$. This range has been explored for mechanically alloyed amorphous FeNbB alloys, where the presence of remaining α-Fe crystallites yields the behavior of the exponent n of the system to deviate from the field independency predicted for single phase materials [22].
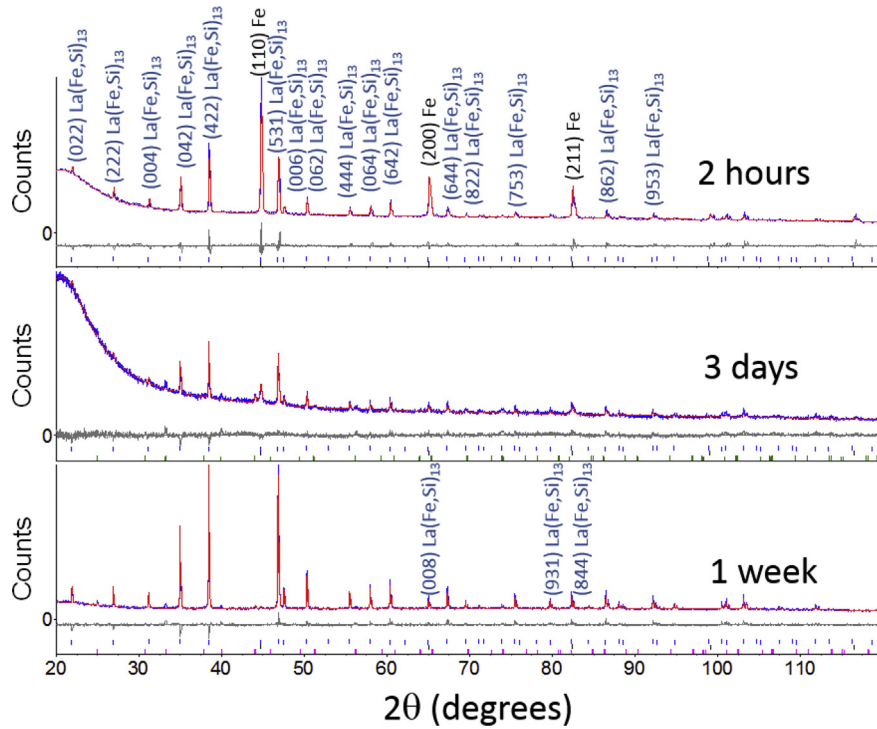
Fig. 1. XRD patterns (blue) and theoretical spectra generated by Rietveld refinement (red) of the three studied samples. (For interpretation of the references to colour in this figure legend, the reader is referred to the web version of this article.)

Table 1
Parameters obtained from XRD and Mössbauer spectroscopy for the studied samples: X_{XRD} and X_{MS}, fractions of α-Fe phase from XRD and Mössbauer, respectively; a_{fcc} and a_{bcc}, lattice parameters of the fcc La(Fe,Si)$_{13}$ phase and the bcc α-Fe(Si) phase, respectively; $<HF>$, average hyperfine magnetic field of the α-Fe(Si) phase.

As-cast sample	Time at 1323 K	X_{XRD} (w. %)	a_{fcc} (Å)	a_{bcc} (Å)	X_{MS} (at. %)	$<HF>$ (T)
Ingot	1 week	1.3	11.4725(1)	2.8646(13)	2.8	32.5(1.0)
Ingot	3 days	24.4	11.4738(7)	2.8659(4)	34.0	32.4(1.1)
Ribbon	2 h	55.8[a]	11.4762(4)	2.8662(1)	54.1	31.7(1.6)

[a] Textured sample.

Finally if $T << T_C^{(1)}$ and $T >> T_C^{(2)}$, then $n_1 = 1$ and $n_2 = 2$ and Eq. (3) can be written as:

$$n\left(T_C^{(2)} << T << T_C^{(1)}\right) = \frac{a_1 X H + 2a_2(1-X)H^2}{\Delta S_M} \qquad (7)$$

And after regrouping the terms

$$\frac{n\Delta S_M}{H} = a_1 X + 2a_2(1-X)H \qquad (8)$$

In order to estimate the temperature range in which these approximations (where we assign $n_1 = 1$ and/or $n_2 = 2$ as the phase's exponent) are valid, the magnetic entropy change of individual phases was simulated using Brillouin functions. In order to do so, we imposed the Curie temperatures, the average magnetic moment per Fe atom and the numerical density of magnetic moments of each phase (1000 K, 2.2 μB and 8.5·10^{28} m^{-3} for α-Fe phase and 250 K, 2.1 μB [23] and 6.1·10^{28} m^{-3} for LaFe$_{11.5}$Si$_{1.5}$, respectively). The local field exponent n was then calculated as a function of both the field change and the temperature difference to the Curie temperature, $\Delta T = T - T_C$. Fig. 4 shows the simulated $n(H)$ curves for different ΔT values and it can be observed that, for paramagnetic samples ($\Delta T > 0$) at $\Delta H = 1.5$ T, the error of assuming $n = 2$ is less than 1% for $\Delta T \geq 30$ K and, for ferromagnetic samples ($\Delta T < 0$) at $\Delta H = 1.5$ T, the error of assuming $n = 1$ is less than 1% only after $|\Delta T| > 100$ K.

There are several features which simplify the analysis in the temperature range $T << T_C^{(1)}$ and $T >> T_C^{(2)}$, leading to equation (8): the exponents of the two phases are no longer free parameters but known and the behavior is not affected by the type of transformation (first or second order) but only by the magnetic state of the phase (ferromagnetic or paramagnetic). In fact, in the case of the LaFe$_{11.5}$Si$_{1.5}$ phase (phase 2 in our study) a first order phase transition occurs due to a volume change of the unit cell at a temperature T_t [24]. However, in order to use $n_2 = 2$, we are only concerned about the paramagnetic phase that exists above this transition temperature with $T_C \leq T_t$. The main disadvantage is that the recorded signal is far from the transition and thus weak.

Therefore, experimental $\Delta S_M(T,H)$ curves were measured clearly above the transition temperature of LaFe$_{11.5}$Si$_{1.5}$ and well below the expected Curie temperature of the α-Fe(Si) phase: from 350 to 475 K, which lies well into the region of validity predicted with $\Delta T \geq 100$ K for the paramagnetic phase and $|\Delta T| > 500$ K for the ferromagnetic phase. In fact the lattice parameter measured for the α-Fe(Si) phase [25] and the average hyperfine magnetic field measured by Mössbauer [26] spectroscopy correspond to a low Si content (~5 at.%) with a high T_C(α-Fe(Si))>1000 K. Fig. 5 shows n
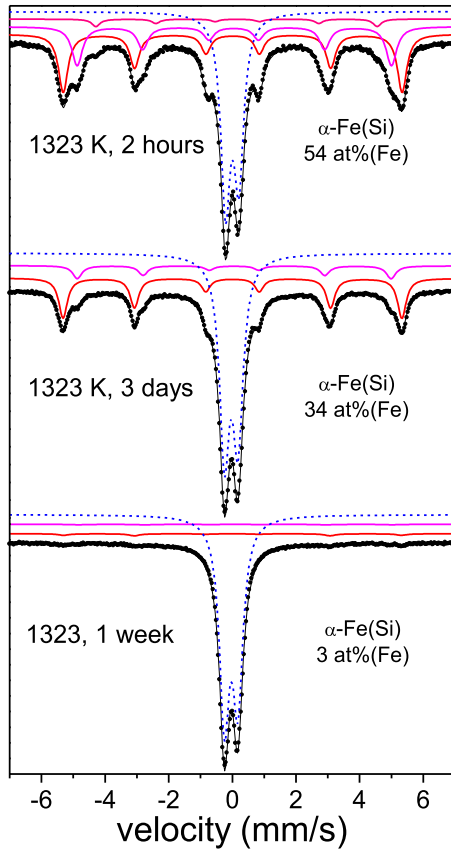
Fig. 2. Mössbauer spectra and contributions used to fit them for the three studied samples.

Fig. 4. Theoretical exponent n calculated using Brillouin functions to describe the magnetization and using a $T_C = 1000$ and 250 K, a magnetic moment of 2.2 and 2.1 μ_B, and a numerical density of magnetic moments of $8.5 \cdot 10^{28}$ and $6.1 \cdot 10^{28}$ m^{-3} for α-Fe (ferromagnetic range) and LaFe$_{11.5}$Si$_{1.5}$ phases (paramagnetic range) respectively.

values in the analyzed temperature range. Fig. 6 shows the plots of $n\Delta S_M/H$ as a function of H for different temperatures for each studied sample. As predicted by Eq. (8), the plots can be fitted to straight lines and the different values of the slope $m(X,T)$ and the intercept $b(X,T)$ are obtained as a function of transformed fraction and temperature. These dependencies can be explicitly stated as follows:

$$m(X,T) = 2a_2(T)(1-X) \tag{9}$$

$$b(X,T) = a_1(T)X \tag{10}$$

From the intercept $b(X,T)$, assuming its average value in the temperature range explored for each sample (in order to reduce the errors), we get an average $<a_1>X$ value that could be compared to the data obtained from XRD and Mössbauer. Fig. 7 shows $<a_1>X$ vs. the α-Fe fraction for the studied samples using both microstructural techniques. Results are in agreement showing that MCE response in

Fig. 3. Magnetic entropy change at 1.5 T for the three studied samples in the temperature range of the first order phase transition. The inset shows the isothermal magnetization curves for the sample annealed 3 days.
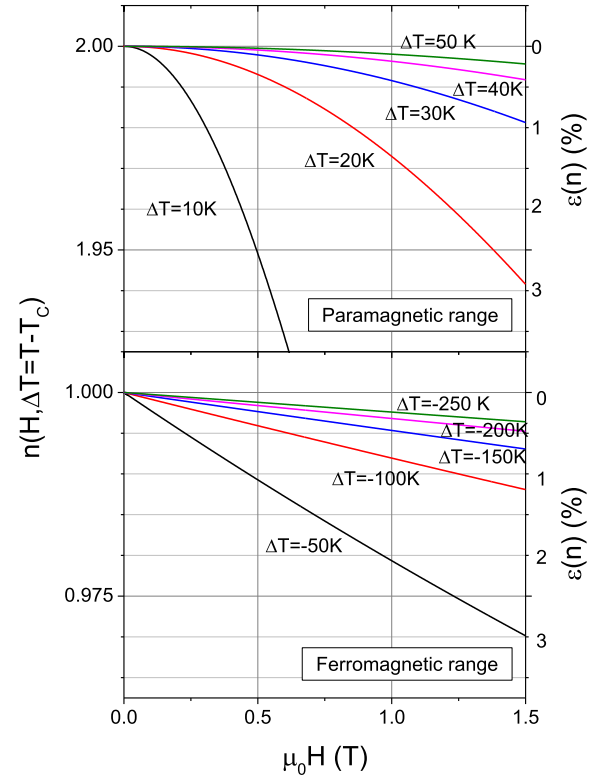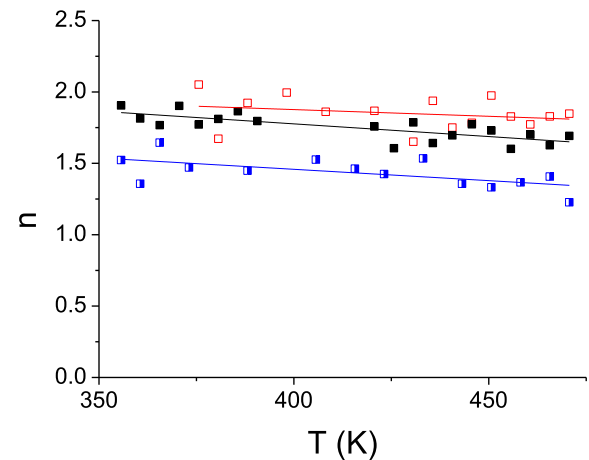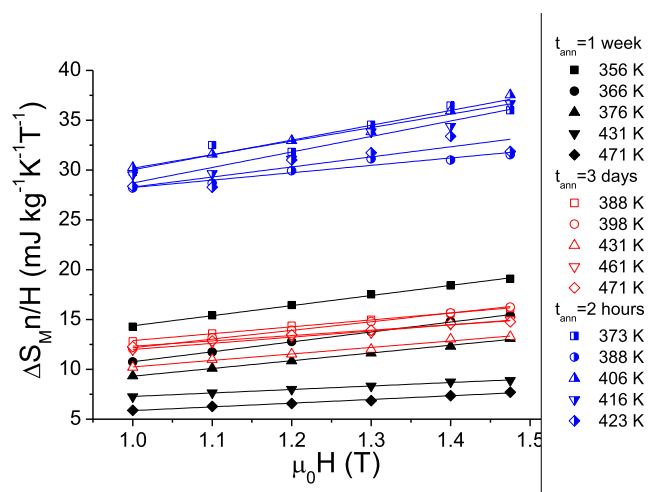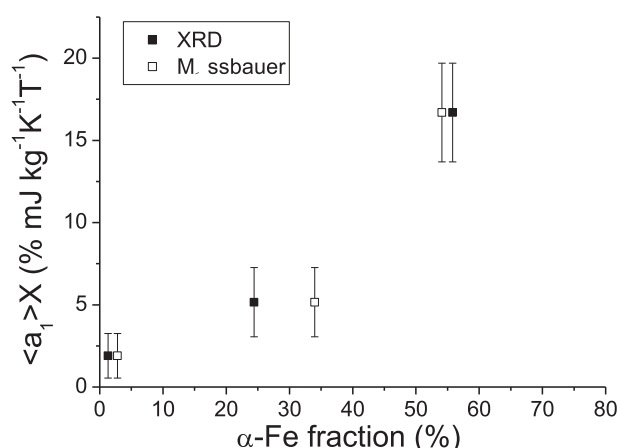

Fig. 5. Experimentally obtained local exponent n at 1.5 T as a function of temperature for the three studied samples. The lines are linear fit to the data.

Fig. 6. Linear dependence of $\Delta S_M n/H$ vs. magnetic field for the three studied samples at some selected temperatures.

Fig. 7. Fraction of α-Fe phase obtained from the analysis of MCE curves vs. that obtained from microstructural observations.

this temperature range can be described by two non-interacting phases which follow a linear field dependence for the α-Fe phase and a quadratic field dependence for the La(Fe,Si)$_{13}$ phase.

In the case of the slope $m(X,T)$, the temperature dependence of a_2 (the magnetic entropy change of the paramagnetic phase at $\Delta H = 1$ T) is stronger than for a_1 (the magnetic entropy change of the ferromagnetic phase at $\Delta H = 1$ T). In fact a Curie–Weiss law could be proposed to describe the decrease of a_2 with the temperature. However, the large errors prevent further discussion on this parameter.

4. Conclusions

The validity of the power law dependence of the magnetic entropy change as a function of field far away from the transition temperature is tested in a composite material formed by fcc La(Fe,Si)$_{13}$ and bcc α-Fe(Si) phases. Results indicate that a non-interacting phases approximation yields satisfactory agreement with microstructural results obtained from different techniques.

The temperature ranges for which the exponent n is almost constant are estimated as a function of the field change. Considering 1% as the error limit, for a field change of 1.5 T, whereas the paramagnetic constant value $n = 2$ is reached a few tens of kelvin above the transition temperature, the ferromagnetic constant value $n = 1$ is only reached after a few hundreds of kelvin below the transition.

The results presented here can be used in the deconvolution of the contribution of impurities to the MCE signal of the main phase with transition around room temperature when the transition temperatures of the impurities are well apart (typically α-Fe crystallites with a $T_C > 1000$ K).

References

[1] V.K. Pecharsky, K.A. Gschneidner Jr., Phys. Rev. Lett. 78 (1997) 4494–4497.
[2] A. Planes, L. Mañosa, M. Acet, J. Phys. Cond. Matter 21 (2009) 233201.
[3] A. Fujita, S. Fujieda, K. Fukamichi, Y. Yamazaki, Y. Iijima, Mater. Trans. 42 (2002) 1202–1204.
[4] H. Wada, Y. Tanabe, Appl. Phys. Lett. 79 (2001) 3302.
[5] M.P. Annaorazov, K.A. Asatryan, G. Myalikgulyev, S.A. Nikitin, A.M. Tishin, A.L. Tyurin, Cryogenics 32 (1992) 867–872.
[6] Gschneidner Jr., V. Pecharsky, Ann. Rev. Mater. Sci. 30 (2000) 387–429.
[7] V. Franco, J.S. Blázquez, B. Ingale, A. Conde, Ann. Rev. Mater. Res. 42 (2012) 305–342.
[8] J. Lyubina, O. Gutfleisch, M.D. Kuzmin, M. Richter, J. Mag. Mag. Mater. 321 (2009) 3571–3577.
[9] M. Phejar, V. Paul-Boncour, L. Bessais, Intermetallics 18 (2010) 2301–2307.
[10] R. Welter, G. Venturini, B. Malaman, J. Alloy Compd. 189 (1992) 49–58.
[11] R. Caballero-Flores, V. Franco, A. Conde, K.E. Knipling, M.A. Willard, Appl. Phys. Lett. 98 (2011) 102505.
[12] S.C. Paticopoulos, R. Caballero-Flores, V. Franco, J.S. Blázquez, A. Conde, K.E. Knipling, M.A. Willard, Solid State Compd. 152 (2012) 1590–1594.
[13] J.S. Blázquez, V. Franco, A. Conde, Intermetallics 26 (2012) 52–56.
[14] H. Osterreicher, F.T. Parker, J. Appl. Phys. 55 (1984) 4336.
[15] V. Franco, J.S. Blázquez, A. Conde, Appl. Phys. Lett. 89 (2006) 222512.
[16] V. Franco, B.C. Dodrill, C. Radu, Magnetics Business & Technology, Winter 2014, 13 (2014) 8.
[17] The analysis software and accompanying Application Note is available at: http://www.lakeshore.com/products/Vibrating-Sample-Magnetometer/Pages/MCE.aspx.
[18] L. Tocado, E. Palacios, R. Burriel, J. Appl. Phys. 105 (2009) 093918.
[19] K. Niitsu, S. Fujieda, A. Fujita, R. Kainuma, J. Alloy Compd. 578 (2013) 220–227.
[20] X.B. Liu, Z. Altounian, D.H. Ryan, J. Phys. Condens. Mater. 15 (2003) 7385–7394.
[21] V. Franco, R. Caballero-Flores, A. Conde, Q.Y. Dong, H.W. Zhang, J. Mag. Mag. Mater. 321 (2009) 1115–1120.
[22] J.J. Ipus, L.M. Moreno-Ramírez, J.S. Blázquez, V. Franco, A. Conde, Appl. Phys. Lett. 105 (2014) 172405.
[23] G.J. Wang, F. Wang, N.L. Di, B.G. Shen, Z.H. Cheng, J. Mag. Mag. Mater. 303 (2006) 84–91.
[24] B.G. Shen, J.R. Sun, F.X. Hu, H.W. Zhang, Z.H. Cheng, Adv. Mater. 21 (2009) 4545–4564.
[25] "Fe-Si (Iron-silicon)" in Springer Materials, The Landolt Bornstein Database, Springer (New Series V).
[26] L. Häggström, L. Gränäs, R. Wäppling, S. Devanarayanan, Phys. Scr. 7 (1973) 125–131.